J Mater Sci (2022) 57:21000–21008

Ceramics

Design of high energy-storage properties in eco-friendly $AgNbO_3$-based ceramics via two-step sintering method and tuning phase boundary

Wenjun Cao[1], Tianyu Li[1,*], Cen Liang[1], and Chunchang Wang[1,*]

[1] Laboratory of Dielectric Functional Materials, School of Physics & Materials Science, Anhui University, Hefei 230601, China

Received: 28 August 2022
Accepted: 10 November 2022
Published online:
20 November 2022

ABSTRACT

Ceramic samples $AgNb_{0.85}Ta_{0.15}O_3$ (ANTO15) and $Ag_{0.85}Bi_{0.05}NbO_3$ (ABNO5) were obtained by two-step sintering method. Dielectric spectra revealed that the M1–M2 and M2–M3 phase boundaries were adjusted to room temperature for ANTO15 and ABNO5, respectively. The ABNO5 sample exhibits pure perovskite phase structure with small grain size, dense, and uniform microstructure. Most importantly, superior comprehensive energy-storage performances of a large recoverable energy-storage density value $\sim$ 3.53 J/cm^3, high energy-storage efficiency $\sim$ 86%, high power density $\sim$ 73.57 MW/cm^3, as well as good energy-storage stabilities were obtained in the ABNO5 ceramic. Our results indicate that the combinative utilization of tuning phase boundary and two-step sintering method gives a feasible method to prepare high energy-storage properties $AgNbO_3$-based eco-friendly ceramic capacitors.

Introduction

Dielectric energy-storage ceramic capacitors characterized by ultrafast charge–discharge speed, long lifetime, and high power density have received global attentions in recent years [1]. But the low energy-storage density greatly limits their application in real life and production [2]. In general, for dielectric energy-storage materials, the recoverable energy-storage density (W_{rec}) and energy-storage efficiency (η) are obtained by the polarization–electric field (*P-E*) hysteresis loop as following [3]:

$$W_{rec} = \int_{Pr}^{P\max} E dP \tag{1}$$

$$\eta = W_{rec}/(W_{rec} + W_{loss}) \tag{2}$$

where E presents the electric field, P_{max} is the saturation polarization, and P_r means the remnant polarization as well. In addition, the W_{loss} equals the area surrounded by the hysteresis loop. Antiferroelectric (AFE) ceramics have been considered to hold tremendous promise for energy-storage application

Handling Editor: David Cann.

Address correspondence to E-mail: jameslty1991@ahpu.edu.cn; ccwang@ahu.edu.cn

Springer

https://doi.org/10.1007/s10853-022-07964-5

due to their double *P-E* loops [4]. However, most AFE ceramics with high energy-storage density contain lead element [5, 6], which is harmful for human health and environment. Thus, there is an ongoing need for exploring novel lead-free AFE energy-storage ceramics. In recent years, Zhao et al. reported that $AgNbO_3$ lead-free ceramic showed the typical antiferroelectric behavior of double *P-E* loops and high energy-storage density [7]. However, pure $AgNbO_3$ ceramic still exhibits the shortcomings of low values of breakdown electric field (E_B) and η. In order to solve the problems, the optimizing preparation technologies have been performed in an effort to improve the E_B value of pure $AgNbO_3$ ceramic [8, 9]. In our previous work, we have confirmed that pure $AgNbO_3$ ceramic with fine-grained and dense microstructure can be prepared by a simple two-step sintering method. This structure feature gives rise to enhanced breakdown field strength. Nevertheless, the two-step sintering method has no obvious influence on the phase transition temperature and energy-storage efficiency of pure $AgNbO_3$ ceramic [9]. Currently, the common method for adjusting phase transition temperature and improving energy-storage efficiency of the pure $AgNbO_3$ ceramic is element-doping at the A- or B-sites [10, 11].

Based on these backgrounds, it is believed that combinative utilization of tuning phase boundary and two-step sintering method would contribute to superior comprehensive energy-storage properties of $AgNbO_3$ ceramics. Therefore, element -doping at A- or B-sites was used aiming at tuning the phase boundaries of $AgNbO_3$ ceramics. Two groups $AgNbO_3$-based ceramic samples, namely $AgNb_{0.85}Ta_{0.15}O_3$ (abbreviated as ANTO15) and $Ag_{0.85}Bi_{0.05}NbO_3$ (abbreviated as ABNO5), were designed. According to Refs. 10 and 11, ANTO15 and ABNO5 should show M1–M2 and M2–M3 phase transitions at room temperature, respectively. Meanwhile, the two groups of samples were prepared by two-step sintering method with the purpose to achieve boosted E_B in these samples. A schematic diagram of this novel approach to obtain excellent energy-storage properties of $AgNbO_3$-based lead-free ceramics is clearly displayed in Fig. 1.

Experimental

The experimental procedure for the synthesis of the ceramics and property measurements are described in the Supplementary files.

Results and discussion

Figure 2A and b shows the temperature-dependent dielectric properties measured at various frequencies of the ANTO15 and ABNO5 ceramics. Consistent with our design goals, the M1–M2 and M2–M3 phase boundaries were adjusted to room temperature for the ANTO15 and ABNO5, respectively. The dielectric properties of ABNO5 also exhibit excellent temperature stability. This material would be a novel Class II dielectrics for multilayer ceramic capacitors (MLCC) applications. To corroborate this point, the dielectric constant variations of $\Delta\varepsilon'/\varepsilon'_{25^\circ C}$@50, 100, and 500 kHz in the temperature range of − 100–250 °C are calculated and presented in Fig. 3a. The variations in dielectric constant within 15% with low loss less than 0.01 (seen in Fig. 3b) can be achieved over the temperature range of − 100–196 °C. This finding demonstrates that the ABNO5 ceramic meets the requirements for X8R capacitors.

Figure 4a and b presents *P-E* loops of both samples measured at room temperature. The ANTO15 sample shows double loops, characterizing the typical antiferroelectric feature. The W_{rec} and η values under the measured electric field of 28 kV/mm were calculated to be 4.2 J/cm^3 and 72%, respectively, which are better than those of the sample prepared by one-step sintering method in other work [10]. As seen from Fig. 4b, the ABNO5 ceramic sample does not show a square-shaped *P-E* curve similar to that of $AgNbO_3$-based ceramics reported in the past. It shows a slim *P-E* curve, which is similar to that of relaxor antiferroelectrics reported before [12]. As is well known, in AgNbO3-based ceramics, the M1 phase shows metastable AFE characteristic under applied electric field, leading to a large P_r value. On the other hand, the M2 and M3 phases are regarded as two disordered AFE phases. As a result, relaxor characteristic with slim *P-E* loop is expected if M2–M3 phase transition temperature moves downward to room temperature, which can decrease P_r value and enhance energy-storage properties. Under the tested electric field of 37 kV/mm, W_{rec} was deduced to be

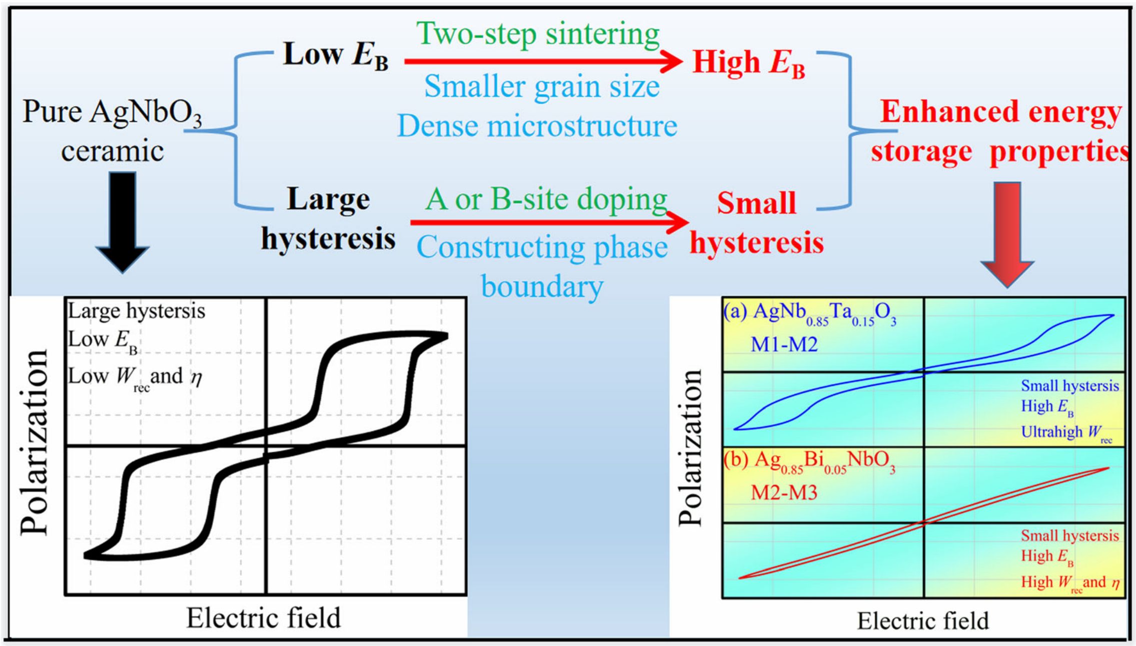

Figure 1 A schematic diagram of the approach to obtain excellent energy-storage properties of $AgNbO_3$-based lead-free ceramics.

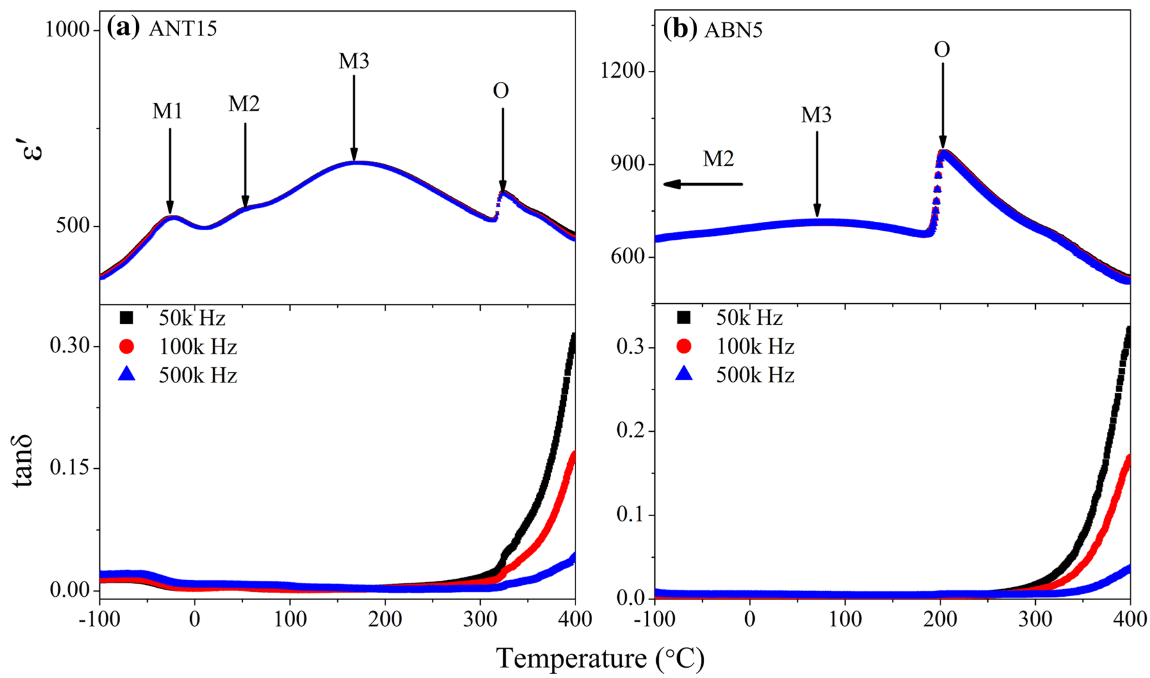

Figure 2 Temperature-dependent dielectric properties of **a** ANTO15 and **b** ABNO5.

3.53 J/cm^3 and η = 86%. This fact demonstrates that high values of W_{rec} and η are simultaneously achieved in the ABNO5 ceramic. It can be seen from Figs. S1 and S2 that both samples in this work exhibit pure perovskite and dense microstructure. Compared with ANTO15 sample, the ABNO5 sample has smaller average grain size (2.48 μm). It is well known that small grain size, homogeneous, and dense microstructure can significantly improve the dielectric breakdown strength [1]. For the present samples, the W_{rec} value of the ABNO5 ceramic is somewhat smaller than that of the ANTO15. But the η value of

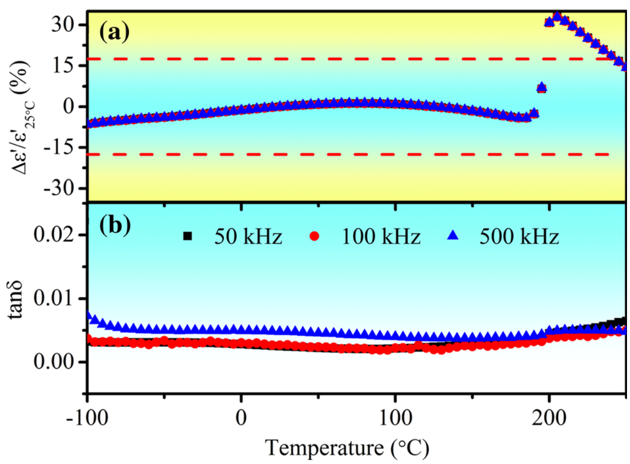

Figure 3 (a) Dielectric constant variation normalized to that at 25 °C and (b) corresponding loss tangent of ABNO5 over the temperature range of − 100–250 °C.

the ABNO5 ceramic is much higher than that of the ANTO15. Furthermore, Fig. 4c displays a comparison of the energy-storage properties between the ABNO5 sample and a large number of other energy-storage ceramics reported recently in literature [11, 13–41]. We can clearly see that the energy-storage properties of ABNO5 sample are much better than most of them.

Additionally, Fig. 5a presents the *P-E* loops of the ABNO5 ceramic measured at 25 kV/mm and 10 Hz in a wide temperature range of 20–100°C. Slim *P-E* loops can be observed in the measured temperature range. The calculated W_{rec} values are shown in Fig. 5b, which reveals that the W_{rec} values are fluctuating between 1.67 and 1.69 J/cm^3. The *P-E* loops of the ABNO5 ceramic measured at 25 kV/mm and room temperature in the frequency range of 1–s200 Hz are also shown in Fig. 5c. Correspondingly, the calculated W_{rec} (1.67 ~ 1.7 J/cm^3) and η (90 ~ 96%) also maintain stable values in the frequency range as shown in Fig. 5d, which means that the ABNO5 sample also possesses excellent temperature and frequency stabilities for energy-storage

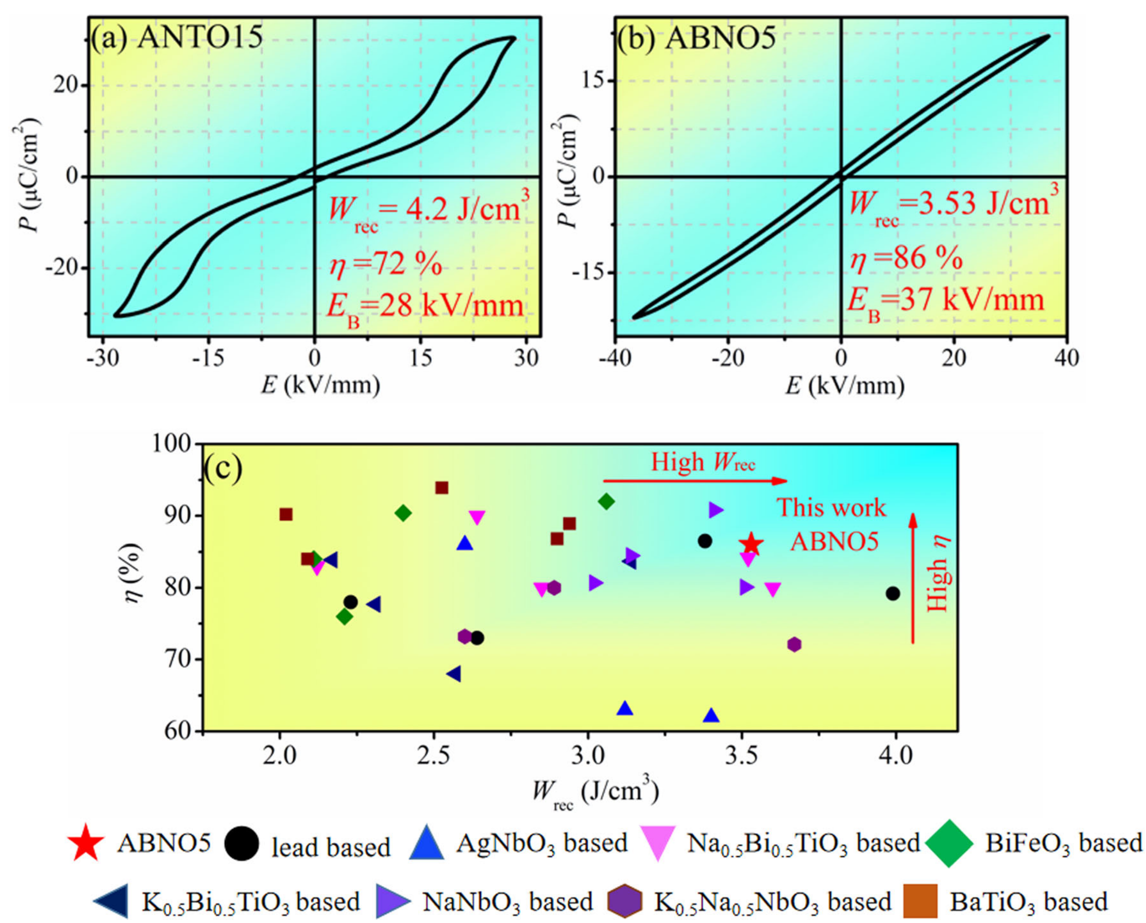

Figure 4 *P-E* loops of **a** ANTO15, **b** ABNO5, and **c** comparison of energy-storage properties between the ABNO5 sample and some other dielectric ceramics.

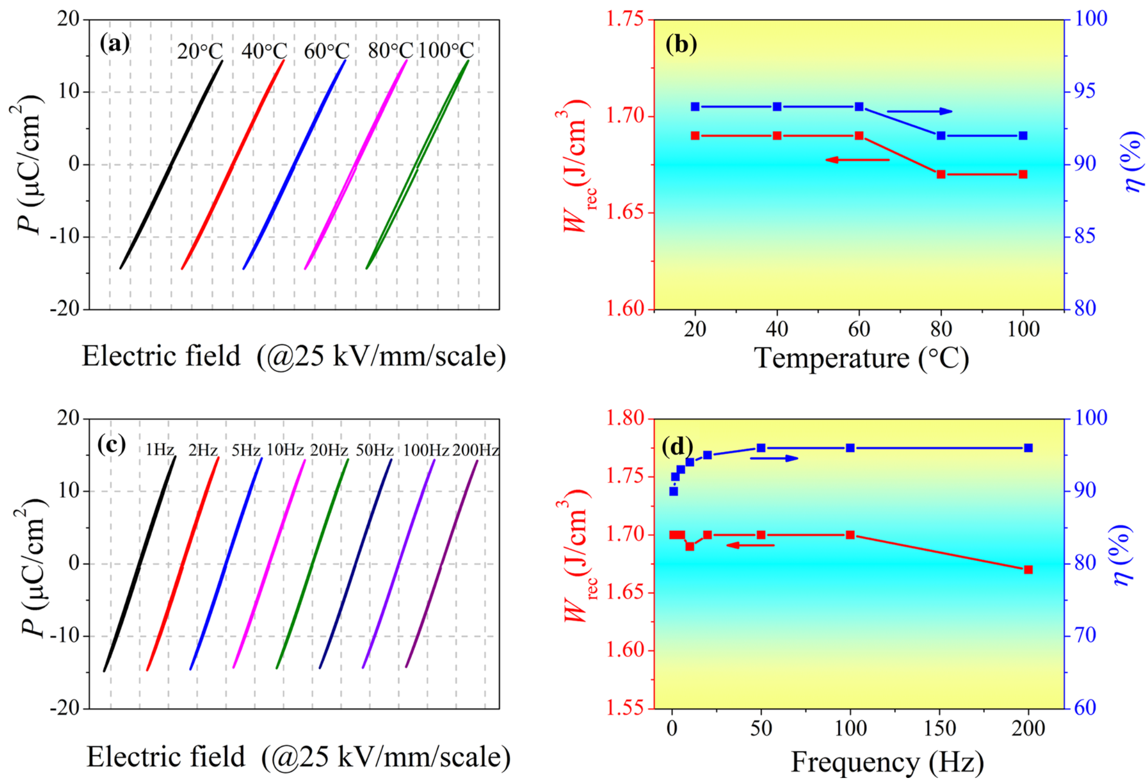

Figure 5 **a** *P-E* loops of the ABNO5 ceramic measured at 25 kV/mm and 10 Hz in the temperature range of 20–100 °C, **b** W_{rec} and η values as a function of temperature, **c** *P-E* loops of the ABN5 ceramic measured at 25 kV/mm and room temperature in the frequency range of 1–200 Hz, and **d** W_{rec} and η values as a function of frequency.

performances. All the features underscore that the ABNO5 sample possesses superior comprehensive energy-storage properties suitable for device application.

Figure 6a shows the undamped pulsed current curves of the ABNO5 ceramic under various electric fields measured at room temperature. The current peak increases as the electric field increases. Under an applied electric field of 20 kV/mm, the maximum current value of 23.1 A can be obtained. The current density (C_D) and power density (P_D) can be calculated as follows [42, 43]:

$$C_D = I_{max}/S \tag{3}$$

$$P_D = EI_{max}/2S \tag{4}$$

where E and S represent the electric field and electrode area, respectively. According to the above

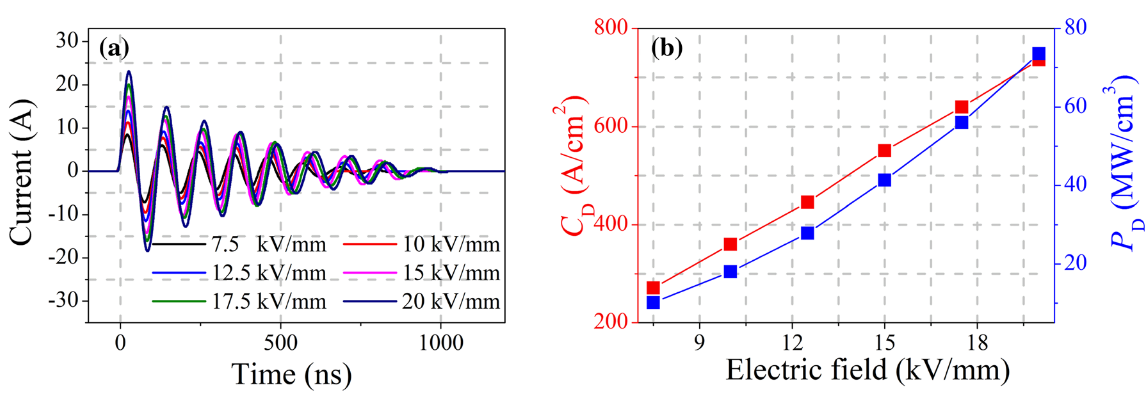

Figure 6 **a** Undamped pulsed current curves under various electric fields, and **b** C_D and P_D as a function of electric field of the ABNO5 ceramic.

Table 1 A comparison between the P_D values of ABNO5 ceramic and other dielectric energy-storage ceramics published in literature [9, 44–49]

Samples	P_D (MW/cm^3)	Ref
$Ag_{0.85}Bi_{0.05}NbO_3$	73.57	This work
$AgNbO_3$	25.7	[9]
$Sr_2Ag_{0.2}Na_{0.8}Nb_{4.7}Ta_{0.3}O_{15}$	70.21	[44]
$0.84Bi_{0.52}Na_{0.48}TiO_3$-$0.16KNbO_3$	66	[45]
$0.9(Sr_{0.7}Bi_{0.2})TiO_3$-$0.1Bi(Mg_{0.5}Zr_{0.5})O_3$	62.6	[46]
$0.9(0.76Bi_{0.5}Na_{0.5}TiO_3$-$0.24SrTiO_3)$-$0.1Bi(Ni_{2/3}Nb_{1/3})O_3$	49.8	[47]
$0.9(0.75BaTiO_3$-$0.25Na0.5Bi0.5TiO_3)$-$0.1Bi(Zn_{0.2}Mg_{0.2}Al_{0.2}Sn_{0.2}Zr_{0.2})O_3$	34.76	[48]
$Ag_{0.97}Nd_{0.01}NbO_3$	54	[49]

formulas, the C_D and P_D values obtained under various electric fields are shown in Fig. 6b. The ABNO5 ceramic has a high power density value P_D = 73.57 MW/cm^3 at 20 kV/mm. Furthermore, it can be found in Table 1 that the P_D value of the ABNO5 ceramic is far greater than to those of other dielectric energy-storage ceramics [9, 44–49]. The high W_{rec} combined with high P_D in the ABNO5 ceramic suggests its promising application potential in pulsed power system.

Conclusions

In this work, ANTO15 and ABNO5 ceramics were successfully prepared via two-step sintering method. Both samples show high W_{rec} values. Excitingly, superior comprehensive energy-storage properties of large W_{rec} (3.53 J/cm^3), high η (86%), and ultrahigh power density (73.57 MW/cm^3) were achieved in ABNO5 sample. Furthermore, ABNO5 sample also has excellent dielectric temperature stability meeting the requirements for X8R capacitors. All above results indicate that the ABNO5 ceramic has great potential for the applications of pulsed power systems.

Acknowledgements

The authors acknowledge financial support from the National Natural Science Foundation of China (Grant Nos. 51872001), Scientific Research Starting Foundation of Anhui Polytechnic University of China (2021YQQ031), the Natural Science Foundation of Anhui Polytechnic University (Grant No. Xjky2022029), and the Open Research Fund Program of the Key Laboratory of Functional Materials and Devices for Informatics of Anhui Higher Education Institutes, Fuyang Normal University (Grant No. FDMI202105).

Declarations

Conflict of interest The authors declare that they have no conflict of interest.

Supplementary Information: The online version contains supplementary material available at https://doi.org/10.1007/s10853-022-07964-5.

References

[1] Yang LT, Kong X, Li F, Hao H, Cheng ZX, Liu HX, Li JF, Zhang SJ (2019) Perovskite lead-free dielectrics for energy storage applications. Prog Mater Sci 102:72–108

[2] Li TY, Jiang XW, Li J, Xie AW, Fu J, Zuo RZ (2022) Ultrahigh energy-storage performances in lead-free $Na_{0.5}Bi_{0.5}TiO_3$-based relaxor antiferroelectric ceramics through synergistic design strategy. ACS Appl Mater Interfaces 14:22263–22269

[3] Li TY, Qiao ZL, Zuo RZ (2022) X9R-type $Ag_{1-3x}Bi_xNbO_3$ based lead-free dielectric ceramic capacitors with excellent energy-storage properties. Ceram Int 48:2533–2537

[4] Han K, Luo NN, Jing Y, Wang XP, Peng BL, Liu LJ, Hu CZ, Zhou HF, Wei YZ, Chen XY, Feng Q (2019) Structure and energy storage performance of Ba-modified $AgNbO_3$ lead-free antiferroelectric ceramics. Ceram Int 45:5559–5565

[5] Liu Z, Lu T, Ye JM, Wang GS, Dong XL, Withers R, Liu Y (2018) Antiferroelectrics for energy storage applications: a Review. Adv Mater Technol 3:1800111

[6] Hao XH, Zhai JW, Kong LB, Xu ZK (2014) A comprehensive review on the progress of lead zirconate-based antiferroelectric materials. Prog Mater Sci 63:1–57

[7] Zhao L, Liu Q, Zhang SJ, Li JF (2016) Lead-free $AgNbO_3$ anti-ferroelectric ceramics with an enhanced energy storage performance using MnO_2 modification. J Mater Chem C 4:8380–8384

[8] Ren PR, Ren D, Sun L, Yan FX, Yang S, Zhao GY (2020) Grain size tailoring and enhanced energy storage properties of two-step sintered Nd^{3+}-doped $AgNbO_3$. J Eur Ceram Soc 40:4495–4502

[9] Li TY, Cao WJ, Chen PF, Wang JS, Wang CC (2021) Effects of sintering method on the structural, dielectric and energy storage properties of $AgNbO_3$ lead-free antiferroelectric ceramics. J Mat Sci 56:13499–13508. https://doi.org/10.1007/s10853-021-06148-x

[10] Zhao L, Liu Q, Gao J, Zhang SJ, Zhang JF (2017) Lead-free antiferroelectric Sliver Niobate Tantalate with high energy storage performance. Adv Mater 29:1701824

[11] Tian Y, Jin L, Zhang HF, Xu Z, Wei XY, Viola G, Abrahams I, Yan HX (2017) Phase transitions in bismuth-modified silver niobate ceramics for high power energy storage. J Mater Chem A 5:17525–17531

[12] Luo NN, Han K, Cabral MJ, Liao XZ, Zhang SJ, Liao CZ, Zhang GZ, Chen XY, Feng Q, Li JF, Wei YZ (2020) Constructing phase boundary in $AgNbO_3$ antiferroelectrics: pathway simultaneously achieving high energy density and efficiency. Nat Commun 11:4824

[13] Luo NN, Han K, Liu LJ, Peng BL, Wang XP, Hu CZ, Zhou HF, Feng Q, Chen XY, Wei YZ (2019) Lead-free $Ag_{1-3x}La_xNbO_3$ antiferroelectric ceramics with high energy storage density and efficiency. J Am Ceram Soc 102:4640–4647

[14] Li L, Wang RX, Zhang ST (2020) Thermally stable energy storage properties in relaxor BNT-6BT-modified antiferroelectric PNZST ceramics. J Am Ceram Soc 103:5769–5777

[15] Liu P, Zhang YJ, Zhu YW, Fan BY, Li WR, Zhang HB, Jiang SL (2019) Structure variation and energy storage properties of acceptor-modified PBLZST antiferroelectric ceramics. J Am Ceram Soc 102:1912–1920

[16] Qiao PX, Zhang YF, Chen XF, Zhou MX, Yan SG, Dong XL, Wang GS (2019) Enhanced energy storage properties and stability in $(Pb_{0.895}La_{0.07})(Zr_xTi_{1-x})O_3$ antiferroelectric ceramics. Ceram Int 45:15898–15905

[17] Yu YX, Zhang YY, Zou KL, Chen G, Zhang Y, Li H, Lu YM, Zhang QF, He YB (2019) High energy density and efficiency in (Pb, La)(Zr, Sn, Ti)O3 antiferroelectric ceramics with high La3+ content and optimized Sn4+ content. Ceram Int 45:24419–24424

[18] Xu YH, Guo Y, Liu Q, Wang GD, Bai JL, Tian JJ, Lin L, Tian Y (2020) High energy storage properties of lead-free Mn-doped $(1-x)AgNbO_3$-$xBi_{0.5}Na_{0.5}TiO_3$ antiferroelectric ceramics. J Eur Ceram Soc 40:56–62

[19] Li TY, Chen PF, Si RJ, Li F, Guo YM, Wang CC (2020) High energy storage density and efficiency with excellent temperature and frequency stabilities under low operating field achieved in $Ag_{0.91}Sm_{0.03}NbO_3$-modified $Na_{0.5}Bi_{0.5}TiO_3$-$BaTiO_3$ ceramics. J Mater Sci: Mater Electron 31:16928–16937. https://doi.org/10.1007/s10854-020-04249-y

[20] Li TY, Chen PF, Li F, Wang CC (2021) Energy storage performance of $Na_{0.5}Bi_{0.5}TiO_3$-$SrTiO_3$ lead-free relaxors modified by $AgNb_{0.85}Ta_{0.15}O_3$. Chem Eng J 406:127151

[21] Fan PY, Zhang ST, Xu JW, Zang JD, Samart C, Zhang T, Tan H, Salamon D, Zhang HB, Liu G (2020) Relaxor/antiferroelectric composites: a solution to achieve high energy storage performance in lead-free dielectric ceramics. J Mater Chem C 8:5681–5691

[22] Ji SS, Li QJ, Wang DD, Zhu JY, Zeng M, Hou ZP, Fan Z, Gao XS, Lu XB, Li QL, Liu JM (2021) Enhanced energy storage performance and thermal stability in relaxor ferroelectric $(1-x)BiFeO_3$-$x(0.85Ba(Sn_{0.5}Zn_{0.5})O_3)$ ceramics. J Am Ceram Soc 104:2646–2654

[23] Chen ZT, Bu XY, Ruan BX, Du J, Zheng P, Li LL, Wen F, Bai WF, Wu W, Zheng L, Zhang Y (2020) Simultaneously achieving high energy storage density and efficiency under low electric field in $BiFeO_3$-based lead-free relaxor ferroelectric ceramics. J Eur Ceram Soc 40:5450–5457

[24] Sun HN, Wang XJ, Sun QZ, Zhang XX, Ma Z, Guo MY, Sun BW, Zhu XP, Liu QD, Lou XJ (2020) Large energy storage density in $BiFeO_3$-$BaTiO_3$-$AgNbO_3$ lead-free relaxor ceramics. J Eur Ceram Soc 40:2929–2935

[25.] Gao XL, Li Y, Chen JW, Yuan C, Zeng M, Zhang AH, Gao XS, Lu XB, Lia QL, Liu JM (2019) High energy storage performances of $Bi_{1-x}Sm_xFe_{0.95}Sc_{0.05}O_3$ lead-free ceramics synthesized by rapid hot press sintering. J Eur Ceram Soc 39:2331–2338

[26] Chen PF, Li TY, Cao WJ, Cheng C, Wang CC (2021) Simultaneously achieved high energy-storage and superior charge-discharge performance in $K_{0.5}Bi_{0.5}TiO_3$-based lead-free ceramics by A-site defect engineering. J Mater Sci: Mater in Elec 32:12121–12133. https://doi.org/10.1007/s10854-021-05840-7

[27] Zhao P, Tang B, Fang ZX, Si F, Yang CT, Zhang SR (2021) Improved dielectric breakdown strength and energy storage properties in Er2O3 modified $Sr_{0.35}Bi_{0.35}K_{0.25}TiO_3$. Chem Eng J 403:126290

[28] Li F, Hou X, Li TY, Si RJ, Wang CC, Zhai JW (2019) Fine-grain induced outstanding energy storage performance in novel $Bi_{0.5}K_{0.5}TiO_3$-$Ba(Mg_{1/3}Nb_{2/3})O_3$ ceramics via a hot-pressing strategy. J Mater Chem C 7:12127–12138

[29] Li F, Si RJ, Li TY, Wang CC (2020) High energy storage performance and fast discharge speed in dense $0.7Bi_{0.5}K_{0.5}TiO_3$-$0.3SrTiO_3$ ceramics via a novel rolling technology. Ceram Int 46:6995–6998
[30] Zhou MX, Liang RH, Zhou ZY, Dong XL (2019) Achieving ultrahigh energy storage density and energy efficiency simultaneously in sodium niobate-based lead-free dielectric capacitors via microstructure modulation. Inorg Chem Front 6:2148–2157
[31] Shi JP, Chen XL, Sun CC, Pang FH, Chen HY, Dong XY, Zhou XJ, Wang KG, Zhou HF (2020) Superior thermal and frequency stability and decent fatigue endurance of high energy storage properties in $NaNbO_3$-based lead-free ceramics. Ceram Int 46:25731–25737
[32] Zhou MX, Liang RH, Zhou ZY, Yan SG, Dong XL (2018) Novel sodium niobate-based lead-free ceramics as new environment-friendly energy storage materials with high energy density, high power density, and excellent stability, ACS Sustain. Chem Eng 6:12755–12765
[33] Yang ZT, Du HL, Jin L, Hu QY, Wang H, Li YF, Wang JF, Gao F, Qu SB (2019) Realizing high comprehensive energy storage performance in lead-free bulk ceramics *via* designing an unmatched temperature range. J Mater Chem A 7:27256–27266
[34] Li YD, Zhen YH, Wang WX, Fang ZQ, Jia ZL, Zhang JY, Zhong H, Wu JG, Yan YG, Xue QZ, Zhu FY (2020) Enhanced energy storage density and discharge efficiency in potassium sodium niobite-based ceramics prepared using a new scheme. J Eur Ceram Soc 40:2357–2365
[35] Qu BY, Du HL, Yang ZT, Liu QH, Liu TH (2016) Enhanced dielectric breakdown strength and energy storage density in lead-free relaxor ferroelectric ceramics prepared using transition liquid phase sintering. RSC Adv 6:34381–34389
[36] Yang ZT, Du HL, Qu SB, Hou YD, Ma H, Wang JF, Wang J, Wei XY, Xu Z (2016) Significantly enhanced recoverable energy storage density in potassium-sodium niobate-based lead free ceramics. J Mater Chem A 4:13778–13785
[37] Li F, Hou X, Wang J, Zeng HR, Shen B, Zhai JW (2019) Structure-design strategy of 0–3 type $(Bi_{0.32}Sr_{0.42}Na_{0.2})TiO_3$/MgO composite to boost energy storage density, efficiency and charge-discharge performance. J Eur Ceram Soc 39:2889–2898
[38] Shi F, Tang B, Fang ZX, Li H, Zhang SR (2019) Enhanced energy storage and fast charge-discharge properties of $(1-x)BaTiO_3$-$xBi(Ni_{1/2}Sn_{1/2})O_3$ relaxor ferroelectric ceramics. Ceram Int 45:17580–17590
[39] Yuan QB, Li G, Yao FZ, Cheng SD, Wang YF, Ma R, Mi SB, Gu M, Wang K, Li JF, Wang H (2018) Simultaneously achieved temperature-insensitive high energy density and efficiency in domain engineered $BaTiO_3$-$Bi(Mg_{0.5}Zr_{0.5})O_3$ lead-free relaxor ferroelectrics. Nano Energy 52:203–210
[40] Li D, Lin Y, Liu XY, Yang HB, Wang T (2019) Influence of SnO_2 additive on the energy storage properties of $Ba_{0.65}(Bi_{0.5}Na_{0.5})_{0.35}TiO_3$-$SrY_{0.5}Nb_{0.5}O_3$ relaxor ferroelectrics. Ceram Int 45:22625–22631
[41] Huang YL, Zhao CL, Wu B, Wu JG (2020) Multifunctional $BaTiO_3$-based relaxor ferroelectric toward excellent energy storage performance and electrostrictive strain benefiting from crossover region. ACS Appl Mater & Inter 12:23885–23895
[42] Wang J, Li TY, Jiang XW, Zhou C, Xu YJ, Shi RJ, Liu LQ, Chu BJ, Zhao Z, Zuo RZ (2022) An alternative way to design excellent energy-storage properties in $Na_{0.5}Bi_{0.5}TiO_3$-based lead-free system by constructing relaxor dielectric composites. J Eur Ceram Soc 42:6512–6517
[43] Cao WJ, Li TY, Chen PF, Wang CC (2021) Outstanding energy-storage performances in $Na_{0.5}Bi_{0.5}TiO_3$-$BaTiO_3$-$(Sr_{0.85}Bi_{0.1})(Mg_{1/3}Nb_{2/3})O_3$ lead-free ceramics. ACS Appl Energ Mater 4:9362–9367
[44] Xu SD, Hao R, Yan Z, Hou ST, Peng ZH, Wu D, Liang PF, Chao XL, Wei LL, Yang ZP (2022) Enhanced energy storage properties and superior thermal stability in SNN-based tungsten bronze ceramics through substitution strategy. J Eur Ceram Soc 42:2781–2788
[45] Wu LL, Zhang JJ, Du HW, Chen JF, Yu HN, Liu YP, Wang JY, Zhou Y, Yao YX, Zhai JW (2022) Chemical nature of the enhanced energy storage in A-site defect engineered $Bi_{0.5}Na_{0.5}TiO_3$-based relaxor ferroelectrics. J Alloys Compd 905:164183
[46] Hu D, Pan ZB, Tan XY, Yang F, Ding J, Zhang X, Li P, Liu JJ, Zhai JW, Pan H (2021) Optimization the energy density and efficiency of $BaTiO_3$-based ceramics for capacitor applications. Chem Eng J 409:127375
[47] Yang HB, Tian JH, Lin Y, Ma JQ (2021) Realizing ultra-high energy storage density of lead-free $0.76Bi_{0.5}Na_{0.5}TiO_3$–$0.24SrTiO_3$-$Bi(Ni_{2/3}Nb_{1/3})O_3$ ceramics under low electric fields. Chem Eng J 418:129337
[48] Zhou SY, Pu YP, Zhang XQ, Shi Y, Gao ZY, Feng Y, Shen GD, Wang XY, Wang DW (2022) High energy density, temperature stable lead-free ceramics by introducing high entropy perovskite oxide. Chem Eng J 427:131684
[49] Shi P, Wang XJ, Lou XJ, Zhou C, Liu QD, He LQ, Yang S, Zhang XX (2021) Significantly enhanced energy storage properties of Nd^{3+} doped $AgNbO_3$ lead-free antiferroelectric ceramics. J Alloys Compd 877:160162